Synthesis and Anticancer Properties of Water-Soluble Zinc Ionophores

Darren Magda,[1] Philip Lecane,[1] Zhong Wang,[1] Weilin Hu,[1] Patricia Thiemann,[1] Xuan Ma,[1] Patricia K. Dranchak,[2] Xiaoming Wang,[2] Vincent Lynch,[3] Wenhao Wei,[3] Viktor Csokai,[3] Joseph G. Hacia,[2] and Jonathan L. Sessler[3]

[1]Pharmacyclics, Inc., Sunnyvale, California; [2]Department of Biochemistry and Molecular Biology, University of Southern California, Los Angeles, California; and [3]Department of Chemistry and Biochemistry, Institute for Cellular and Molecular Biology, University of Texas at Austin, Austin, Texas

Abstract

Several water-solubilized versions of the zinc ionophore 1-hydroxypyridine-2-thione (ZnHPT), synthesized as part of the present study, have been found both to increase the intracellular concentrations of free zinc and to produce an antiproliferative activity in exponential phase A549 human lung cancer cultures. Gene expression profiles of A549 cultures treated with one of these water-soluble zinc ionophores, PCI-5002, reveal the activation of stress response pathways under the control of metal-responsive transcription factor 1 (MTF-1), hypoxia-inducible transcription factor 1 (HIF-1), and heat shock transcription factors. Additional oxidative stress response and apoptotic pathways were activated in cultures grown in zinc-supplemented media. We also show that these water-soluble zinc ionophores can be given to mice at 100 μmol/kg (300 μmol/m^2) with no observable toxicity and inhibit the growth of A549 lung and PC3 prostate cancer cells grown in xenograft models. Gene expression profiles of tumor specimens harvested from mice 4 h after treatment confirmed the *in vivo* activation of MTF-1–responsive genes. Overall, we propose that water-solubilized zinc ionophores represent a potential new class of anticancer agents. [Cancer Res 2008;68(13):5318–25]

Introduction

The role intracellular free (non–protein bound) zinc plays in regulating cellular functions is of considerable relevance to cancer. For example, increased free zinc has been proposed to stabilize hypoxia-inducible factor-1 (HIF-1) and thus influence processes, such as glycolysis, apoptosis, and angiogenesis (1–4). Moreover, free zinc inhibits thioredoxin reductase (5), a key mediator in the cellular response to oxidative stress that is frequently overexpressed in cancer (6–8). The importance of these targets in tumor development led us to hypothesize that small molecules capable of modulating free zinc levels can serve as anticancer agents.

We have recently found that motexafin gadolinium (MGd; Xcytrin), an expanded porphyrin containing the lanthanide cation gadolinium(III), increases intracellular free zinc levels, enhances the cellular toxicity of zinc, and inhibits cellular bioreductive activity in several human cancer cell lines (1, 5). In fact, the ability of MGd to disrupt cellular zinc homeostasis provides a possible mechanistic explanation for its anticancer activity noted in clinical trials (9). Such considerations have led us to propose that synergistic interactions between MGd and exogenous zinc acetate are important for activity and that these interactions would occur regardless of the means of zinc delivery. Indeed, MGd displayed synergy with the zinc ionophore 1-hydroxypyridine-2-thione (ZnHPT) in an *in vitro* assay measuring bioreductive activity (5).

ZnHPT is commonly used to increase intracellular zinc *in vitro* and has been given p.o. to laboratory animals for toxicity testing and to probe zinc homeostasis *in vivo* (10–13). ZnHPT is extensively used as a bacteriocide and fungicide (14). However, the complex is insoluble in aqueous media and is poorly bioavailable (13). The goals of this study were thus (*a*) to prepare a set of water-solubilized ZnHPT analogues to permit controlled zinc delivery both *in vitro* and *in vivo* and (*b*) to test their biological properties in preclinical models. This would facilitate experiments involving ZnHPT and MGd cotreatments and also allow us to evaluate the general utility of zinc ionophores as novel stand-alone anticancer agents.

Materials and Methods

Materials. The synthesis, characterization, and formulation of all compounds used in this study are described in the supplementary data.

Cells and cell culture reagents. A549 lung cancer and PC3 prostate cancer lines were obtained from the American Type Culture Collection. Unless otherwise indicated, all cell culture reagents were purchased from Invitrogen. Cells were cultured in RPMI 1640 supplemented with 20 mmol/L HEPES, 2 mmol/L L-glutamine, 10% heat-inactivated fetal bovine serum (Hyclone) and antibiotics (200 units/mL penicillin and 200 μg/mL streptomycin).

Cellular and biochemical activity assays. Previously described assays for measuring cell proliferation, thioredoxin reductase activity, the concentration of intracellular free zinc, cell viability, and apoptosis were used in our analyses (1). A detailed description of each assay is provided in the supplementary data.

Gene expression profiling. A549 human lung cancer cells (1×10^5 per T-25 flask in 7 mL complete RPMI 1640) were seeded 7 d before treatment of noncycling plateau phase cultures with drug. Medium was replaced with fresh medium 24 h before treatment. At 4 h before RNA isolation, ionophore PCI-5002 (final concentration, 10 μmol/L), $Zn(OAc)_2$ (final concentration, 25 μmol/L), the combination, or control (5% mannitol) solution was added to the cultures. Each experiment was performed in triplicate. After incubation, all cultures were washed twice with HBSS supplemented with 0.5% bovine serum albumin and total RNA was isolated and subjected to analysis on Human Genome U133 Plus 2.0 Arrays (Affymetrix), as described (1, 8). ArrayAssist software (Stratagene) was used to normalize hybridization signal (RMA algorithm) and to conduct hierarchical clustering analyses

Note: Supplementary data for this article are available at Cancer Research Online (http://cancerres.aacrjournals.org/).

Requests for reprints: Darren Magda, Pharmacyclics, Inc., 995 E. Arques Avenue, Sunnyvale, CA 94085. Phone: 408-774-3318; Fax: 408-774-0340; E-mail: dmagda@pcyc.com.

doi:10.1158/0008-5472.CAN-08-0601

(15). Genes at least 1.5-fold differentially expressed in drug-treated relative to control samples with a Benjamini-Hochberg corrected Student's t test at $P \leq 0.15$ are reported. GeneOntology analyses were conducted using WebGestalt software (16). All scaled fluorescent intensity values and .cel files are available at the National Center for Biotechnology Information Gene Expression Omnibus repository under Series Accession Number Series GSE6972. In addition, all scaled fluorescent intensity values are available in Supplementary Tables S2 (cell culture experiments) and S3 (xenograft model system).

Mouse xenograft models. Details regarding the generation of xenograft tumors in these studies are provided as supplementary data. When the average size of tumors reached ~100 mm^3, mice were randomized by tumor size to treatment groups, typically containing five to eight mice per group. Mice were treated i.v. with two to four doses of zinc ionophore, 80 or 100 μmol/kg (240 or 300 μmol/m^2), on consecutive days. Vehicle control–treated animals received 5% mannitol on the same schedule. Tumor and body weight measurements were performed thrice per week. MGd was given i.p. 1 h before ionophore. For gene expression profiling, mice were treated i.v. with one dose (100 μmol/kg) PCI-5002, PCI-5003, or control vehicle (four mice per group) when the average A549 tumor size reached 500 mm^3. After 4 h, tumors were harvested and snap frozen immediately on dry ice. Tumor tissue was dissected and homogenized in Trizol (Invitrogen), and total RNA was isolated and subjected to gene expression analysis.

Results

Synthesis of water-soluble ionophores. We considered that the solubilization of ZnHPT could be accomplished by attachment of an amphoteric substituent, which would allow it to retain the capacity for diffusion across the cell membrane. To this end, a first water-solubilized version of ZnHPT, bearing a tri(ethyleneglycol)-methyl ether substituent at the 5-position (PCI-5003), was synthesized (Fig. 1*A*). Unlike the parent compound, PCI-5003 was soluble (>12 mmol/L) in 5% aqueous mannitol.

The shorter chain analogues PCI-5001 and PCI-5002 were prepared using analogous synthetic procedures. The corresponding ligands (PCI-5501, PCI-5502, and PCI-5503) were also isolated (Fig. 1*B*). In 5% aqueous mannitol, PCI-5002 was soluble to a level of at least 6 mmol/L. However, PCI-5001 had only limited water solubility (<1 mmol/L in 5% aqueous mannitol). This latter complex was formulated in DMSO and only tested in *in vitro* studies. Nevertheless, we obtained PCI-5001 in single crystalline form (Fig. 1*C*) and measured important bond lengths and angles (Supplementary Table S1). This structure is notably similar to that of ZnHPT (14), providing important support for the conclusion that the modifications made to enhance water solubility do not interfere significantly with the metal ion complexation properties of the 1-hydroxypyridine-2-thione (HPT) core.

Effect of ZnHPT analogues on cellular proliferation. In A549 lung cancer cell proliferation analyses, PCI-5003 displayed an apparent inhibitory concentration higher than that of ZnHPT whereas PCI-5002 and PCI-5001 showed intermediate activity (Fig. 2). The activity of ZnHPT was increased considerably by coincubation with exogenous zinc. In contrast, the activity of PCI-5003 seemed less affected by zinc at the concentrations examined. PCI-5002 and PCI-5001 were progressively more responsive to zinc. Similar trends were observed in PC3 prostate cancer cells (Supplementary Fig. S1).

We next examined the antiproliferative activities of the non-complexed ligands that comprise ZnHPT and its analogues. In general, the antiproliferative activities of these ligands (HPT, PCI-5501, PCI-5502, and PCI-5503) and their corresponding zinc complexes show excellent correlation (cf. Supplementary Fig. S2). This indicates that the antiproliferative activities of the zinc complexes derive in part from the activities of the ligands (Supplementary Fig. S3).

Effect of ZnHPT analogues on cell survival. The effects of ZnHPT and its analogues on the survival of plateau phase cultures after 24-hour treatment were also compared. ZnHPT displayed greater activity than PCI-5003, with PCI-5002 and PCI-5001 showing intermediate activity (Fig. 3*A*). However, in all instances, coincubation with exogenous zinc(II) cation was required for cell death at the complex concentrations tested. The amount of zinc acetate added to the medium raised its concentration to a level (25 μmol/L) roughly equivalent to that present in human plasma (17).

The activities of the ligands (HPT, PCI-5501, PCI-5502, and PCI-5503) were also examined in plateau phase experiments (Fig. 3*B*), and these led to similar levels of cell death, but only when supplemented with zinc. This indicates that the ligands alone are insufficient to cause cell death in plateau phase cultures at the concentrations tested and that the complexes are responsible for the observed biological effects.

Intracellular free zinc measurements. Plateau phase A549 cells were treated with ZnHPT or its analogues, with or without 25 μmol/L exogenous $Zn(OAc)_2$, for 4 hours and analyzed for changes in intracellular free zinc by flow cytometry using the zinc-selective fluorescent probe FluoZin-3 (18). No fluorescent

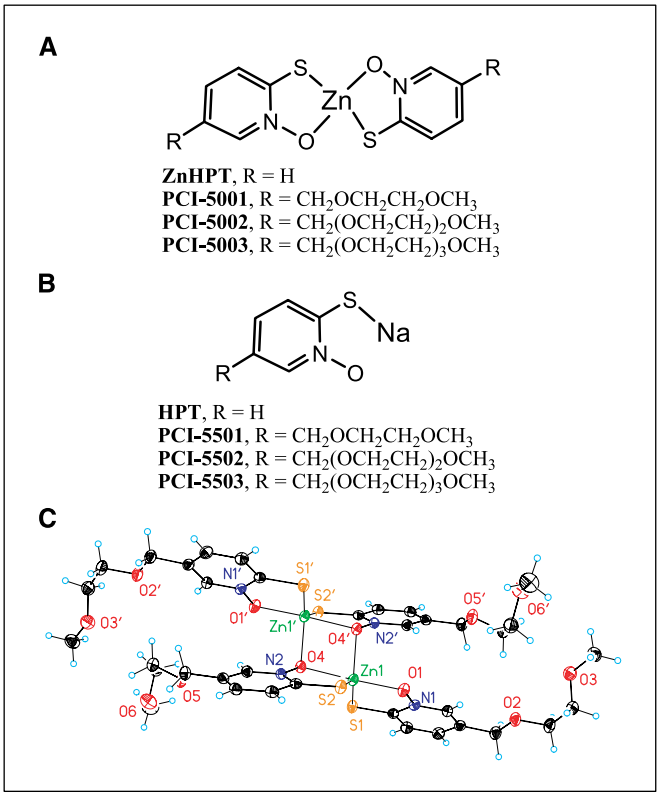

Figure 1. Structures of zinc ionophores used in this study. *A,* structural formula of ZnHPT and water-solubilized complexes. *B,* structural formula of HPT sodium salt and related zinc ligands. *C,* view of the dimeric complex found in PCI-5001 showing the atom labeling scheme. Displacement ellipsoids are scaled to the 50% probability level.

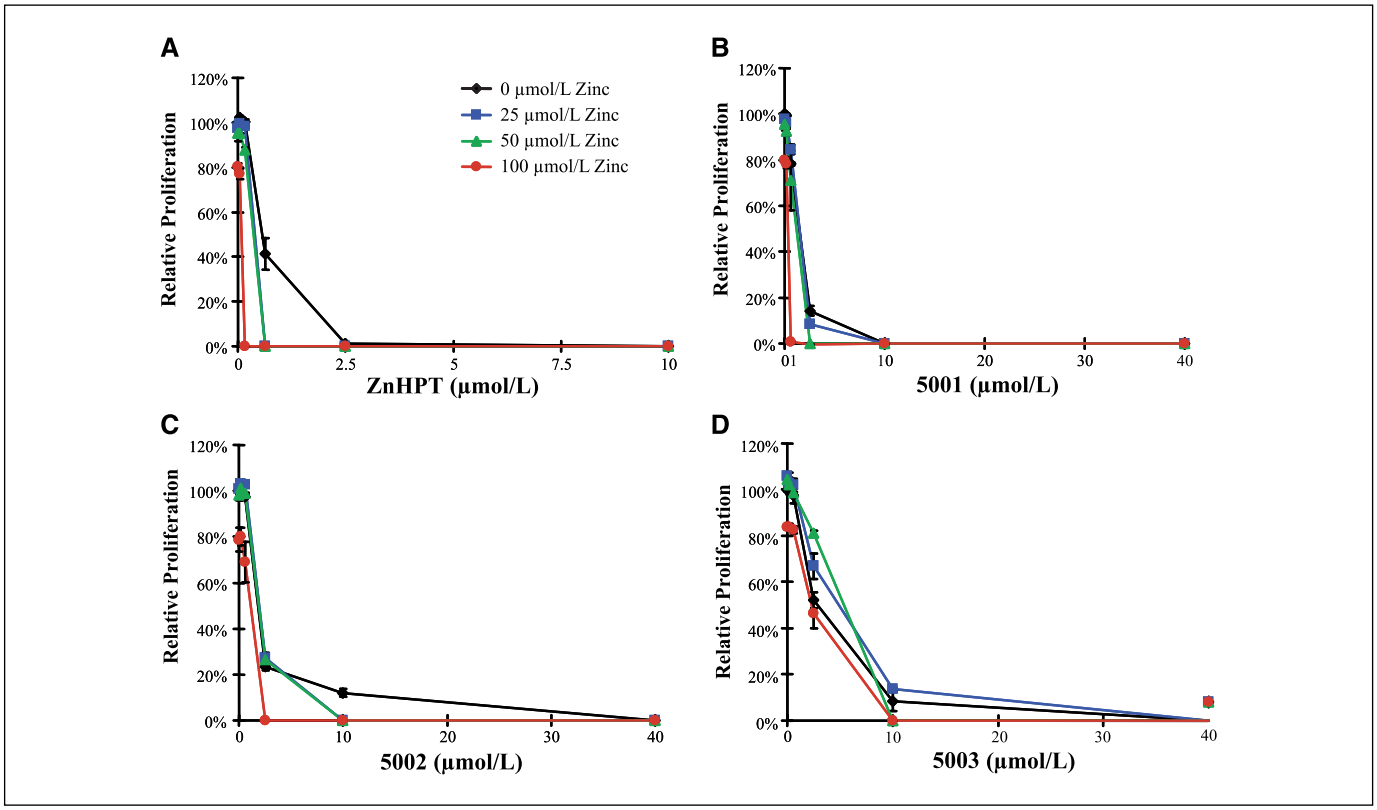

Figure 2. Zinc ionophores inhibit proliferation of A549 cells. Exponential phase A549 cell cultures were treated with zinc complexes (*A–D*) at the indicated concentrations in the presence or absence of zinc acetate [0 μmol/L (*black line*), 25 μmol/L (*blue line*), 50 μmol/L (*green line*), and 100 μmol/L (*red line*)] for 72 h in duplicate experiments. *Error bars,* 1 SD.

changes were observed in live-gated cells treated with 10 μmol/L PCI-5003 (Fig. 3*C*). In contrast, ZnHPT (2.5 μmol/L) led to a slight increase in FluoZin-3 fluorescence even in the absence of exogenous zinc, although this signal was enhanced considerably in its presence. The intensity of the FluoZin-3 signal was enhanced slightly after treatment with PCI-5002 or PCI-5001 (10 μmol/L) in the absence of added zinc, but increased substantially when these complexes were tested in the presence of exogenous zinc. Cultures were also incubated with ZnHPT or its analogues, 25 μmol/L exogenous $Zn(OAc)_2$, and MGd (10 μmol/L) for 4 hours and analyzed for changes in intracellular free zinc (Fig. 3*D*). Taken together, these experiments indicate that the smaller compounds are able to transport zinc and decrease cell viability in zinc-supplemented medium. Even in the presence of exogenous zinc, PCI-5003 (10 μmol/L) failed to facilitate zinc transport significantly. However, it was active at higher zinc concentrations or in the PC3 cell line (cf. Supplementary Fig. S4).

Effect of ZnHPT analogues on lipoate reduction. Increased levels of intracellular free zinc can block cellular reduction of lipoate to form dihydrolipoate, principally by inhibition of thioredoxin reductase (5). In fact, we found that lipoate reduction was inhibited after treatment for 2 hours with ZnHPT analogues and zinc or with MGd in zinc-supplemented medium (cf. Supplementary Figs. S5 and S6). Inhibition of lipoate reduction closely paralleled zinc signal and the cell death observed in cultures treated under like conditions for 24 hours. For example, treatment of A549 cells with 10 μmol/L PCI-5002 with exogenous zinc led to 70% decreased rate of lipoate reduction (Supplementary Fig. S5), a 7-fold increase in zinc signal (Fig. 3*C*), and ~50% cell death (Fig. 3*A*).

Gene expression profiling of cultured A549 cells. To understand better the effect of a zinc ionophore on transcription, gene expression profiles were analyzed in plateau phase A549 cells treated with 10 μmol/L PCI-5002 for 4 hours in normal medium or in medium supplemented with 25 μmol/L exogenous zinc. These conditions were chosen based on the consideration that no cell death was observed in the absence of exogenous zinc, whereas a 50% decrease in viability was measured after 24 hours with zinc supplementation (cf. Fig. 3*A*). All 21 transcripts that were differentially expressed (up-regulation in all cases; >1.5-fold corrected $P < 0.15$) in response to treatment with PCI-5002 in the absence of zinc are listed in Table 1. They include transcripts regulated by metal-responsive transcription factor 1 (MTF-1; e.g., 10 metallothionein-related and 2 zinc transporter transcripts), HIF-1 (i.e., *HMOX1*), and heat shock transcription factors (HSF; e.g., five heat shock–related transcripts).

Experiments conducted with the same (10 μmol/L) dosage of PCI-5002 in zinc-supplemented medium showed 917 differentially expressed transcripts (Supplementary Table S2). GeneOntology (GO) analyses of the 608 up-regulated transcripts showed enrichment (≥4 transcripts, $P < 0.001$) for multiple functional categories, including regulators of transcription, protein folding genes, and mitogen-activated protein kinase phosphatase activity (Supplementary Fig. S7). As one might anticipate, transcripts with cell death–related functions (e.g., *DDIT3, DEDD2*, and *GADD45B*)

were among the most highly induced (>8-fold change, corrected $P < 0.15$). GO analyses of the 309 down-regulated transcripts also showed enrichment (≥4 transcripts, $P < 0.001$) for multiple functional categories, including nuclear mRNA splicing and regulators of transcription (Supplementary Fig. S8). In contrast, no gene expression changes resulting from growth in zinc-supplemented media were seen in the absence of added complex. Furthermore, it was not possible to discriminate between the zinc-treated and control cultures based on hierarchical clustering analysis (Fig. 4). In contrast, the cultures treated with PCI-5002 in standard or zinc-supplemented medium formed distinct groups based on the same analysis.

Toxicity. Single-dose toxicity testing (three mice per cohort) was conducted using PCI-5002 and PCI-5003. Both compounds were found to be well-tolerated at the highest i.v. dose (120 μmol/kg, 360 μmol/m^2) tested. Moderate signs of toxicity (transient inactivity) were observed at the highest dose level, lasting a few minutes longer for PCI-5002 compared with PCI-5003.

Activity in tumor xenograft models. Initial xenograft studies were conducted in CD-1 nude mice bearing A549 lung cancer tumors (19). PCI-5002 and PCI-5003 were given to mice i.v. at a dose level of 100 μmol/kg (300 μmol/m^2) on 4 consecutive days. Although modest growth inhibition was observed initially in animals treated with either zinc complex ($P < 0.05$, days 8–16), this effect did not maintain statistical significance at later times (Fig. 5*A*). A stoichiometric amount (200 μmol/kg) of the corresponding ligand (PCI-5502) did not significantly inhibit tumor growth rate (data not shown). No significant effects on mouse body weight were observed due to treatment.

The effect of combined treatment using PCI-5003 and MGd was also examined. In this study, MGd (40 μmol/kg) was given i.p. 1 hour before ionophore on 2 consecutive days. A slightly lower dosage of ionophore (80 μmol/kg) was used to mitigate possible toxicity resulting from the combined treatment. Treatment with PCI-5003 alone was without effect on tumor growth rate, whereas combined treatment with MGd led to significant tumor growth delay (log-rank test, $P < 0.01$; Fig. 5*B*). No effect on body weight was observed.

The effect of PCI-5002 treatment on the growth of PC3 prostate cancer xenografts was then examined. It was noted previously (5) that PC3 cells are more sensitive than A549 cells to zinc treatment *in vitro*. PCI-5002 was again given i.v. at the 100 μmol/kg dose level. In this instance, a significant tumor growth delay was observed, wherein PCI-5002 was given on 4 consecutive days (log-rank test, $P = 0.02$; Fig. 5*C*). Two-day treatments with PCI-5002 did not significantly inhibit tumor growth, suggesting that more prolonged treatment was required. As before, no effect on body weight due to treatment was observed.

Gene expression profiling of tumor xenografts. A549 tumors, grown as described above, were treated with PCI-5002 (100 μmol/kg), PCI-5003 (100 μmol/kg), or control vehicle when their volume reached 500 mm^3. After 4 hours, tumors (four per cohort) were excised and homogenized, and total RNA was extracted for microarray analysis. Hierarchical clustering of gene expression data showed a separation of drug-treated and control animals (Supplementary Fig. S9). However, the A549 xenografts from PCI-5002–treated and PCI-5003–treated animals yielded similar gene expression profiles based on the same analysis. Table 1 lists all differentially expressed transcripts in response to treatment with PCI-5002 and/or PCI-5003. Interestingly, two

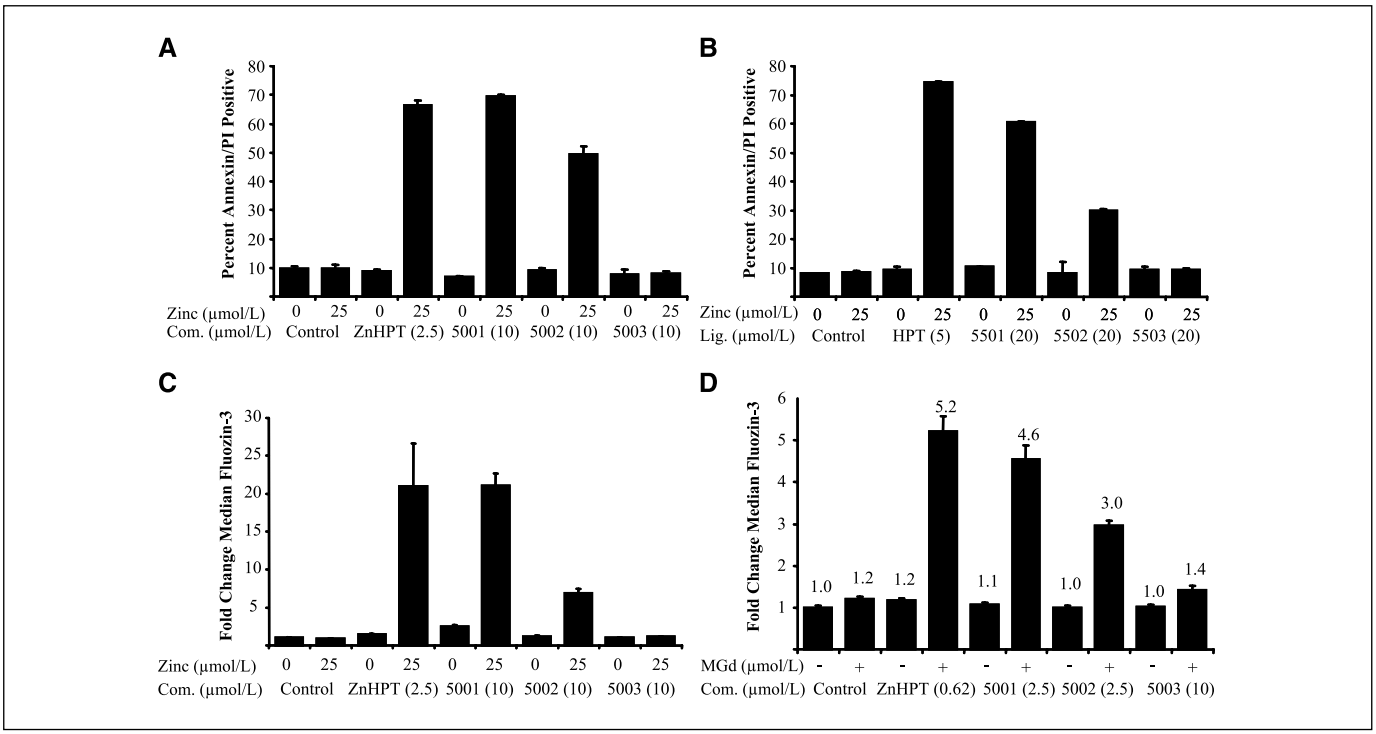

Figure 3. Zinc ionophore treatment alters levels of intracellular free zinc and cell death of A549 cells in response to zinc. Plateau phase A549 cultures were treated with zinc complexes (*Com.*; 2.5 or 10 μmol/L) or zinc ligands (*Lig.*; 5 or 20 μmol/L) in the presence or absence of zinc acetate (*Zinc*; 25 μmol/L) for up to 24 h in duplicate experiments. *Error bars,* 1 SD. *A* and *B,* percentage of Annexin-V/propidium iodide (*PI*)–stained cells after 24 h. *C,* fold increase of FluoZin-3 fluorescence in live-gated cells after 4 h. *D,* fold increase of FluoZin-3 fluorescence in live-gated cells after 4 h treatment with zinc ionophores (2.5 or 10 μmol/L) in the presence or absence of MGd (10 μmol/L) in medium supplemented with zinc acetate (25 μmol/L).

Table 1. Transcriptional responses in A549 cultures and xenografts treated with zinc ionophores

	Probe ID	Gene ID*	Symbol	Gene description	10 μmol/L PCI-5002 †		
					FC	Corrected P ‡	P§
A549 cell cultures	213629_x_at	4494	*MT1F*‖	Metallothionein 1F	19.1	0.0049	5.42×10^{-7}
	210524_x_at	—	—	Similar to metallothionein 1F	13.2	0.0185	3.11×10^{-6}
	217165_x_at	4494	*MT1F*‖	Metallothionein 1F	11.8	0.0023	8.59×10^{-8}
	208581_x_at	4501	*MT1X*‖	Metallothionein 1X	9.7	0.0025	2.06×10^{-7}
	204326_x_at	4501	*MT1X*‖	Metallothionein 1X	9.0	0.0025	2.23×10^{-7}
	206461_x_at	4496	*MT1H*‖	Metallothionein 1H	7.5	0.0095	1.22×10^{-6}
	212185_x_at	4502	*MT2A*‖	Metallothionein 2A	6.8	0.0023	5.31×10^{-8}
	204745_x_at	4495	*MT1G*‖	Metallothionein 1G	6.5	0.0272	5.98×10^{-6}
	211456_x_at	645745	*MT1P2*	Metallothionein 1 pseudogene 2	6.1	0.0234	4.28×10^{-6}
	212907_at	7779	*SLC30A1*‖	Solute carrier family 30 (zinc transporter)	5.0	0.0025	2.29×10^{-7}
	216336_x_at	4499	*MT1K*	Metallothionein 1M	4.4	0.0901	3.73×10^{-5}
	228181_at	7779	*SLC30A1*‖	Solute carrier family 30 (zinc transporter)	4.4	0.0479	1.14×10^{-5}
	200800_s_at	3303	*HSPA1A*‖	Heat shock 70 kDa protein 1A	3.6	0.0901	3.56×10^{-5}
	203665_at	3162	*HMOX1*	Heme oxygenase (decycling) 1	3.0	0.1278	7.87×10^{-5}
	200799_at	3303	*HSPA1A*	Heat shock 70 kDa protein 1A	2.2	0.0901	2.70×10^{-5}
	227124_at	221710	*LOC221710*	Hypothetical protein	1.7	0.0901	3.26×10^{-5}
	218566_s_at	26973	*CHORDC1*	Cysteine and histidine-rich domain containing 1	1.7	0.1371	9.03×10^{-5}
	200881_s_at	3301	*DNAJA1*	DnaJ (Hsp40) homologue, subfamily A	1.6	0.0901	4.12×10^{-5}
	200880_at	3301	*DNAJA1*	DnaJ (Hsp40) homologue, subfamily A	1.6	0.0272	5.82×10^{-6}
	207714_s_at	871	*SERPINH1*	Heat shock protein 47	1.5	0.1467	1.15×10^{-4}
	217911_s_at	9531	*BAG3*	BCL2-associated athanogene 3	1.5	0.1467	1.17×10^{-4}
	Probe ID	Gene ID*	Symbol	Gene description	100 μmol/kg Ionophore †		
					FC	Corrected P ‡	P§
A549 Xenografts PCI-5002	217165_x_at	4494	*MT1F*‖	Metallothionein 1F	1.8	0.1486	2.72×10^{-4}
	206461_x_at	4496	*MT1H*‖	Metallothionein 1H	1.7	0.0633	1.74×10^{-5}
	212185_x_at	4502	*MT2A*‖	Metallothionein 2A	1.7	0.1261	8.05×10^{-5}
	208581_x_at	4501	*MT1X*‖	Metallothionein 1X	1.7	0.1468	2.24×10^{-4}
	212907_at	7779	*SLC30A1*‖	Solute carrier family 30 (zinc transporter)	1.6	0.0512	5.77×10^{-6}
	205097_at	1836	*SLC26A2*	Solute carrier family 26 (sulfate transporter)	1.5	0.1096	5.21×10^{-5}
	204745_x_at	4495	*MT1G*‖	Metallothionein 1G	1.5	0.1486	3.18×10^{-4}
	224941_at	5069	*PAPPA*	Pregnancy-associated plasma protein A	−1.6	0.0192	7.03×10^{-7}
A549 Xenografts PCI-5003	224840_at	2289	*FKBP5*	FK506 binding protein 5	2.2	0.1187	5.38×10^{-5}
	213629_x_at	4494	*MT1F*‖	Metallothionein 1F	1.9	0.1367	5.35×10^{-4}
	217165_x_at	4494	*MT1F*‖	Metallothionein 1F	1.8	0.1433	6.74×10^{-4}
	212907_at	7779	*SLC30A1*‖	Solute carrier family 30 (zinc transporter)	1.6	0.1187	8.35×10^{-5}
	226350_at	1122	*CHML*	Choroideremia-like (Rab escort protein 2)	1.5	0.1325	2.12×10^{-4}
	222529_at	51312	*SLC25A37*	Solute carrier family 25, member 37	−2.5	0.1407	5.84×10^{-4}
	200800_s_at	3303	*HSPA1A*	heat shock 70 kDa protein 1A	−2.1	0.1354	3.14×10^{-4}
	202499_s_at	6515	*SLC2A3*	Solute carrier family 2 (glucose transporter)	−2.0	0.1187	5.28×10^{-5}
	207966_s_at	2734	*GLG1*	Golgi apparatus protein 1	−1.8	0.1456	8.07×10^{-4}
	223161_at	57189	*KIAA1147*	KIAA1147	−1.8	0.1325	1.99×10^{-4}
	227484_at	—	—	CDNA FLJ41690 fis, clone HCASM2009405	−1.7	0.1187	1.08×10^{-4}
	242121_at	51132	*RNF12*	ring finger protein 12	−1.6	0.1354	3.02×10^{-4}
	201454_s_at	9520	*NPEPPS*	Aminopeptidase puromycin sensitive	−1.6	0.1456	7.56×10^{-4}
	200998_s_at	10970	*CKAP4*	Cytoskeleton-associated protein 4	−1.6	0.1276	1.63×10^{-4}
	211962_s_at	677	*ZFP36L1*	Zinc finger protein 36, C3H type-like 1	−1.5	0.1325	2.13×10^{-4}

Abbreviation: FC, fold change.

*Entries with identical National Center for Biotechnology Information Gene ID designations represent results from different probe tilings interrogating the same gene.

† Transcripts with a ≥1.5-fold change relative to untreated control, Benjamini-Hochberg corrected Student's t test $P \leq 0.15$, and the |mean test expression score − mean control expression score| ≥ 100 units are shown.

‡ Benjamini-Hochberg corrected Student's t test.

§ Student's t test.

‖ Gene is differentially expressed in the same direction in both the cell culture and xenograft model(s).

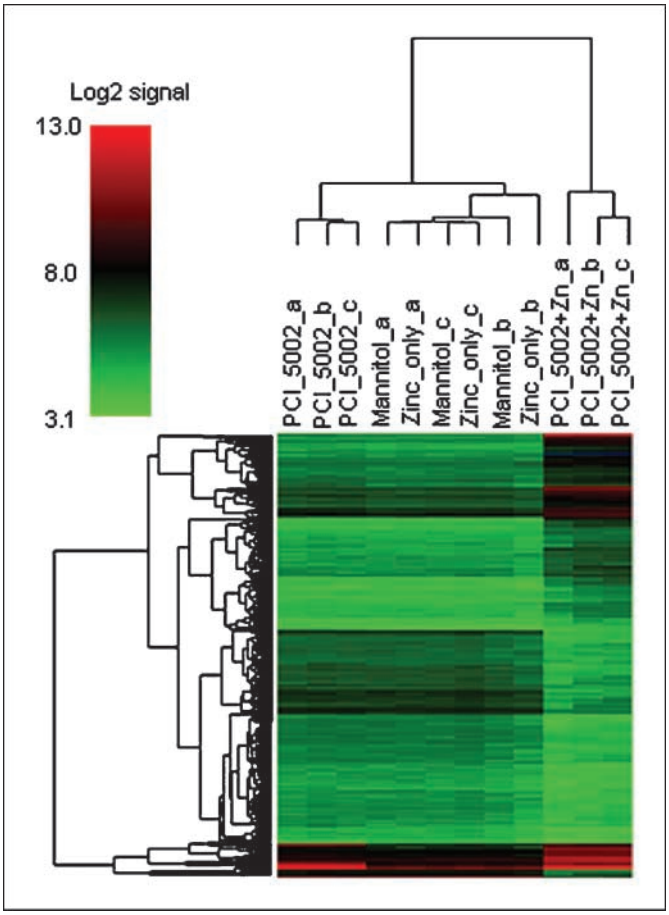

Figure 4. Hierarchical clustering analysis of gene expression data from A549 cell cultures. The dendrograms were generated based on average linkage hierarchical clustering of expression data from 538 transcripts whose coefficient of variation was >0.10 across all *in vitro* groups. Data from untreated (mannitol), zinc-treated (25 μmol/L zinc acetate), PCI-5002–treated (10 μmol/L), and combination-treated (25 μmol/L zinc and 10 μmol/L PCI-5002) A549 cultures are provided in triplicate.

MTF-1–regulated transcripts (i.e., *MT1F* and *SLC30A1*) were up-regulated by both drugs (Table 1). Whereas only one transcript was down-regulated in response to PCI-5002, a total of 10 were down-regulated in response to PCI-5003. However, GO analyses of these 10 transcripts indicated no enrichment for functional categories (≥2 transcripts, $P < 0.001$).

Discussion

Based on the hypothesis that the growth and survival of cancer cells are sensitive to intracellular zinc levels, we sought to prepare compounds that could be used to deliver zinc to tumors. The zinc ionophore ZnHPT inhibits the growth of cancer cells in culture (20), but is not appropriate for parenteral administration, due to its limited solubility in aqueous media. This motivated us to synthesize and characterize solubilized ZnHPT analogues, specifically PCI-5001, PCI-5002, and PCI-5003, bearing mono(ethyleneglycol)methyl ether, di(ethyleneglycol)-methyl ether, and tri(ethyleneglycol)methyl ether substituents, respectively.

PCI-5003 displayed antiproliferative activity *in vitro*, albeit at higher concentrations relative to ZnHPT. Interestingly, in contrast to ZnHPT, the antiproliferative activity of PCI-5003 was not increased by medium supplementation with zinc acetate (Fig. 2). Thus, we concluded that the lower activity of PCI-5003 compared with ZnHPT did not arise solely from a decrease in the stability of the former complex. Rather, it was considered more likely that the larger size of the PCI-5003 inhibits cell uptake. Therefore, we

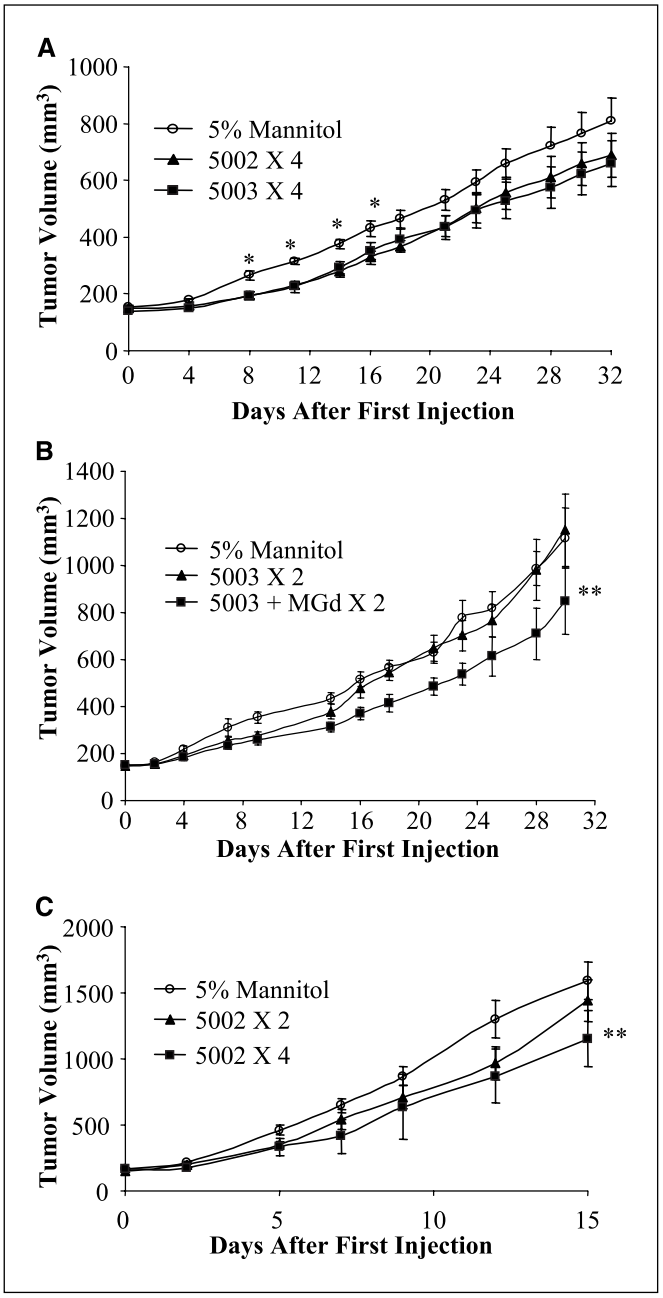

Figure 5. Activity of zinc ionophores in tumor xenograft models. *A,* median tumor volume (±SE) over time in nude mice bearing A549 tumors treated with control (5% mannitol) vehicle, PCI-5002 (100 μmol/kg q.d. × 4), or PCI-5003 (100 μmol/kg q.d. × 4). *, $P < 0.05$, Student's *t* test. *B,* median tumor volume (±SE) over time in nude mice bearing A549 tumors treated with control vehicle, PCI-5003 (80 μmol/kg q.d. × 2), or MGd (40 μmol/kg i.p.) + PCI-5003 (80 μmol/kg q.d. × 2). **, $P < 0.01$, log-rank test, time to 500 mm^3. *C,* median tumor volume (±SE) over time in nude mice bearing PC3 tumors treated with control vehicle, PCI-5002 (100 μmol/kg q.d. × 2), or PCI-5002 (100 μmol/kg q.d. × 4). **, $P = 0.02$, log-rank test, time to 500 mm^3.

prepared the lower molecular weight congeners PCI-5002 and PCI-5001 and found that the *in vitro* activities of these analogues were intermediate between those of PCI-5003 and ZnHPT (Fig. 2).

Ionophore treatment led to cell death in noncycling cultures, albeit at higher concentrations and only in the presence of supplementary zinc (Fig. 3*A*). To rationalize the disparate requirement for zinc supplementation in exponential and plateau phase cultures, it is useful to recognize that we expect partial dissociation of the ionophore into its constituent parts under our conditions. In fact, it has been calculated that a 1 μmol/L ZnHPT solution at pH 7 is composed of 43% unbound zinc, 43% zinc bound by one ligand, and only 14% intact complex (14). Thus, we propose that the observed antiproliferative activities of ZnHPT or its analogues are largely due to unbound ligands that interfere with cellular processes by binding metals. In fact, the ligands alone displayed antiproliferative properties similar to those found for the complexes (Supplementary Fig. S2). In plateau phase cultures, effective concentrations tend to be higher and zinc dependent, consistent with participation of the intact zinc complex as the biologically active species. This interpretation is supported by the observation that cell death in plateau phase cultures correlates with increased intracellular free zinc levels (Fig. 3*A*–*C*).

Cotreatment of the cultures with ionophore and MGd provides an additional means of assessing the level and importance of zinc transport into the cells. Based on previous work (5), MGd would be expected to increase cellular toxicity, inhibit lipoate reduction, and increase FluoZin-3 fluorescence under conditions where the intracellular free zinc concentration was increased via application of an ionophore. Indeed, in medium supplemented with 25 μmol/L zinc, a synergistic effect of MGd on FluoZin-3 fluorescence is apparent for all ZnHPT analogues (Fig. 3*D*).

In the present study, we observe increased expression of transcripts under the control of MTF-1, HIF-1, and HSFs after treatment with PCI-5002 in normal (i.e., zinc deficient) RPMI 1640. Widespread transcriptional activation and repression was observed in cells treated with PCI-5002 and grown in media supplemented with an approximate physiologic concentration (25 μmol/L) of exogenous zinc. Notably, robust proapoptotic transcriptional responses were observed under these conditions.

PCI-5002 and PCI-5003 were sufficiently soluble in aqueous media to permit i.v. administration and testing in A549 and PC3 xenograft models. A549 tumor growth was inhibited transiently by both agents (Fig. 5*A*). Since we had shown that MGd would potentiate the effects of zinc *in vitro* (5), we also examined the effect of i.p. treatment with MGd, followed after 1 hour by PCI-5003. MGd treatment alone does not significantly inhibit A549 tumor growth (Supplementary Fig. S10). However, in combination with PCI-5003, we observed significant tumor growth inhibition (Fig. 5*B*). In the PC3 model, tumor growth was inhibited significantly by treatment using PCI-5002 after four doses, but not after two doses (Fig. 5*C*). This leads us to suggest that more effective tumor control might be observed after more prolonged treatment or in combination with MGd.

Growth inhibitory effects were not seen when a stoichiometric amount of the ligand corresponding to PCI-5002 (data not shown) was used. This leads us to propose that the effects of PCI-5002 are due to enhanced delivery of zinc to tumors, rather than a consequence of metal ion chelation within the tumors by the unbound ligand. Unfortunately, such controls are difficult to interpret due to possible differences in the biodistribution of such ligands relative to their corresponding zinc complex. Therefore, we measured the effect of PCI-5002 and PCI-5003 on gene expression levels in A549 xenografts to confirm the ionophore activity of these compounds *in vivo*. In tumors harvested 4 hours after administration with either compound, we observed increased expression levels of MTF-1–regulated transcripts, such as metallothioneins and zinc transporter 1 (Table 1). Such a finding is consistent with the zinc ionophores serving to effect zinc delivery into the tumors.

Tumor growth inhibition in rodents has been reported consequent to chronic zinc administration using an implanted device or with the zinc ionophore clioquinol (21, 22). Increased levels of intracellular free zinc activate survival pathways but can lead to cell cycle arrest and cell death under conditions where adaptive response mechanisms are overwhelmed. Under the hypoxic and hypoglycemic conditions present in tumors, responses to these stresses may be particularly important due to metabolic adjustments made by cancer cells to adapt to their environment. Consequently, the zinc ionophores described in this report may display a preferential effect in tumor cells. If correct, this conjecture would support further development of agents that provide a sustained delivery of zinc to tumors. This approach may be particularly germane in prostate cancer, given the unusually high zinc levels normally found in this tissue and lost upon transformation (17, 21).

Disclosure of Potential Conflicts of Interest

D. Magda: employment and ownership interest, Pharmacyclics, Inc.; Z. Wang: employment, Pharmacyclics, Inc.; X. Ma: employment, Pharmacyclics, Inc.; P. K. Dranchak: commercial research grant, Pharmacyclics, Inc.; X. Wang: commercial research grant, Pharmacyclics, Inc.; J.G. Hacia: commercial research grant, Pharmacyclics, Inc. The other authors disclosed no potential conflicts of interest.

Acknowledgments

Received 2/15/2008; revised 3/28/2008; accepted 4/9/2008.

Grant support: NIH grant CA68682 (J.L. Sessler) and Rosztoczy Foundation postdoctoral fellowship (V. Csokai). Part of this investigation was conducted in a facility constructed with support from Research Facilities Improvement Program grant C06 (RR10600-01, CA62528-01, RR14514-01) from National Center for Research Resources, NIH.

The costs of publication of this article were defrayed in part by the payment of page charges. This article must therefore be hereby marked *advertisement* in accordance with 18 U.S.C. Section 1734 solely to indicate this fact.

References

1. Lecane PS, Karaman MW, Sirisawad M, et al. Motexafin gadolinium and zinc induce oxidative stress responses and apoptosis in B-cell lymphoma lines. Cancer Res 2005;65:11676–88.
2. Hirsila M, Koivunen P, Xu L, Seeley T, Kivirikko KI, Myllyharju J. Effect of desferrioxamine and metals on the hydroxylases in the oxygen sensing pathway. FASEB J 2005;19:1308–10.
3. Schofield CJ, Ratcliffe PJ. Oxygen sensing by HIF hydroxylases. Nat Rev Mol Cell Biol 2004;5:343–54.
4. Semenza GL. Targeting HIF-1 for cancer therapy. Nat Rev Cancer 2003;3:721–32.
5. Magda D, Lecane P, Miller RA, et al. Motexafin gadolinium disrupts zinc metabolism in human cancer cell lines. Cancer Res 2005;65:3837–45.
6. Smart DK, Ortiz KL, Mattson D, et al. Thioredoxin

reductase as a potential molecular target for anticancer agents that induce oxidative stress. Cancer Res 2004;64: 6716–24.
7. Choi JH, Kim TN, Kim S, et al. Overexpression of mitochondrial thioredoxin reductase and peroxiredoxin III in hepatocellular carcinomas. Anticancer Res 2002;22: 3331–5.
8. Kirkpatrick DL, Kuperus M, Dowdeswell M, et al. Mechanisms of inhibition of the thioredoxin growth factor system by antitumor 2-imidazolyl disulfides. Biochem Pharmacol 1998;55:987–94.
9. Mehta MP, Rodrigus P, Terhaard CH, et al. Survival and neurologic outcomes in a randomized trial of motexafin gadolinium and whole-brain radiation therapy in brain metastases. J Clin Oncol 2003;21: 2529–36.
10. Gibson WB, Jeffcoat AR, Turan TS, Wendt RH, Hughes PF, Twine ME. Zinc pyridinethione: serum metabolites of zinc pyridinethione in rabbits, rats, monkeys, and dogs after oral dosing. Toxicol Appl Pharmacol 1982;62:237–50.
11. Jeffcoat AR, Gibson WB, Rodriguez PA, Turan TS, Hughes PF, Twine ME. Zinc pyridinethione: urinary metabolites of zinc pyridinethione in rabbits, rats, monkeys, and dogs after oral dosing. Toxicol Appl Pharmacol 1980;56:141–54.
12. Jasim S, Tjalve H. Effect of zinc pyridinethione on the tissue disposition of nickel and cadmium in mice. Acta Pharmacol Toxicol (Copenh) 1986;59:204–8.
13. Jasim S, Tjalve H. Effects of sodium pyridinethione on the uptake and distribution of nickel, cadmium and zinc in pregnant and non-pregnant mice. Toxicology 1986;38: 327–50.
14. Doose CA, Ranke J, Stock F, Bottin-Weber U, Jastorff B. Structure-activity relationships of pyrithiones-IPC-81 toxicity tests with the antifouling biocide zinc pyrithione and structural analogs. Green Chem 2004;6:259–66.
15. Wang Z, Lecane PS, Thiemann P, et al. Synthesis and biologic properties of hydrophilic sapphyrins, a new class of tumor-selective inhibitors of gene expression. Mol Cancer 2007;6:9.
16. Zhang B, Kirov S, Snoddy J. WebGestalt: an integrated system for exploring gene sets in various biological contexts. Nucleic Acids Res 2005;33 (Web Server issue): W741–8.
17. Costello LC, Franklin RB. Novel role of zinc in the regulation of prostate citrate metabolism and its implications in prostate cancer. Prostate 1998;35: 285–96.
18. Gee KR, Zhou ZL, Ton-That D, Sensi SL, Weiss JH. Measuring zinc in living cells. A new generation of sensitive and selective fluorescent probes. Cell Calcium 2002;31:245–51.
19. Sirotnak FM, Zakowski MF, Miller VA, Scher HI, Kris MG. Efficacy of cytotoxic agents against human tumor xenografts is markedly enhanced by coadministration of ZD1839 (Iressa), an inhibitor of EGFR tyrosine kinase. Clin Cancer Res 2000;6:4885–92.
20. Gibson WT, Chamberlain M, Parsons JF, et al. The effect and mode of action of zinc pyrithione on cell growth. I. *In vitro* studies. Food Chem Toxicol 1985;23: 93–102.
21. Feng P, Li TL, Guan ZX, Franklin RB, Costello LC. Effect of zinc on prostatic tumorigenicity in nude mice. Ann N Y Acad Sci 2003;1010:316–20.
22. Ding WQ, Liu B, Vaught JL, Yamauchi H, Lind SE. Anticancer activity of the antibiotic clioquinol. Cancer Res 2005;65:3389–95.